J Appl Electrochem (2013) 43:817–827
DOI 10.1007/s10800-013-0572-z

ORIGINAL PAPER

Nb as an influential element for increasing the CO tolerance of PEMFC catalysts

Thairo A. Rocha · Felipe Ibanhi · Flávio Colmati · José J. Linares · Valdecir A. Paganin · Ernesto R. Gonzalez

Received: 9 February 2013 / Accepted: 4 June 2013 / Published online: 18 June 2013

Abstract Platinum–niobium catalysts were prepared as candidates for CO tolerant anode catalysts for low and high temperature PEM fuel cells (PEMFCs). Three different compositions were prepared by the formic acid method, from platinum (hexachloroplatinic acid) and niobium (niobium chloride) precursors on Vulcan XC-72R carbon black. Deposition of the niobium was found to be quite difficult, and only a fraction of the desired composition was achieved. Mean particle sizes were all in the nanometric range, between 2 and 3 nm. Diffraction patterns display neither insertion of niobium within the crystalline structure of platinum, nor any crystalline phase associated to that material. Nevertheless, the presence of Nb displays a noticeable effect on the CO tolerance of the catalyst firstly revealed by a reduction of the CO stripping onset potential. Fuel cell results, operating with Nafion® at low temperature (80 °C) and H_2 + 100 ppm of CO as fuel, and with H_3PO_4-doped ABPBI, at high temperature (150 °C) and H_2 + 20,000 ppm of CO, display an enhancement in the performance compared to pure platinum, so niobium may be an interesting material for increasing the tolerance to carbon monoxide in PEMFC. Finally, CO/O_2 polarisation curves display a decrease in the current density in the presence of Nb, confirming that the enhanced CO tolerance can be attributed to a strong electronic effect that weakens the Pt–CO adsorption strength.

Keywords PEMFC · CO tolerance · Niobium · Low temperature · High temperature

T. A. Rocha · F. Ibanhi · V. A. Paganin · E. R. Gonzalez (✉)
Institute of Chemistry of São Carlos, University of São Paulo, Av. Trabalhador SãoCarlense, 400, CP 780, São Carlos, São Paulo CEP 13560-970, Brazil
e-mail: ernesto@iqsc.usp.br

F. Colmati
Institute of Chemisty, Federal University of Goiás, CP 131, Goiânia, Goiás CEP 74001-970, Brazil

J. J. Linares
Institute of Chemistry, University of Brasília, CP 4478, Brasília, Distrito Federal CEP 70910-000, Brazil

1 Introduction

Polymer electrolyte membrane fuel cells (PEMFCs) have been suggested as attractive energy conversion systems due to their high efficiency for the direct conversion of the energy contained in a fuel into electricity [1]. Compared to the main competitors, fuel cells can produce energy continuously provided that the fuel is supplied, whilst batteries are subjected to charge/discharge cycles due to the depletion of the reactants [2]. Traditional PEMFCs are fed with hydrogen in the anode (although other fuels such as alcohols are possible), and oxygen in the cathode. Although the final product is water, harmless to the environment and oxygen is available from atmospheric air, hydrogen is just an energy vector, not freely available in nature. Therefore, it has to be produced from primary power sources [3]. The ideal scenario would be possible if this fuel is "cleanly" produced from renewable sources, and two primary ways have been proposed:

- Coupling of renewable energy sources (solar-photovoltaic and windmills) with an electrolysis/hydrogen storage/fuel cell system. During low demand periods, the excess energy is used to produce hydrogen, and subsequently stored. Then, during high demand periods, the fuel cell can give back the stored energy [4].

- Hydrogen can be produced from the catalytic reforming of hydrocarbons or alcohols. In this sense, Brazilian economy possesses a well-developed ethanol production and distribution network, and hence, ethanol reforming can be a strategic route for producing hydrogen [5].

Ethanol reforming is a well-established process in which, under ideal conditions, syngas ($H_2 + CO$) is obtained. The main problem associated to this potential fuel for fuel cells is the presence of carbon monoxide. It strongly adsorbs on the platinum based catalysts used in the fuel cell, resulting in a blockade of the active sites. A dramatic decrease of the cell performance is then observed for temperatures below 80 °C in Nafion®-based PEMFC systems if tens of ppm of CO are present in the gas.

In order to address this issue, several approaches have been proposed: (i) a strict cleaning in order to reduce the CO content of the syngas [6]; (ii) development of better CO tolerant anode catalysts for the fuel cell, aiming at reducing the complexity of the CO cleaning system. This research group has been developing such type of catalysts. Bimetallic platinum-based catalysts have been synthesised based on the combination of that metal with less noble metals, such as ruthenium [7], tin [8], molybdenum [9], tungsten [7, 10], osmium [11], forming alloys, segregated metallic phases, or in the form of oxides. The physical and morphological characteristics of the prepared catalysts were studied and the electrochemical performance in the presence of carbon monoxide was determined; (iii) increase of the operating temperature, on the basis of the negative value of the CO adsorption entropy on platinum [12]. However, in this case, high temperature resistant membrane materials are necessary [13]. Examples are the polybenzimidazoles (PBI) impregnated with phosphoric acid, particularly, the poly[2,2-(*m*-phenylene)-5,5-bibenzimidazole] (*m*-PBI) and the poly(2,5-benzimidazole) (ABPBI), whose conductivity, chemical stability and thermal resistance fulfil all the requirements [14, 15]. Therefore, the use of a PBI-based high temperature PEMFC could be an interesting approach to deal with the presence of CO. Furthermore, a more attractive system could be implemented by combining a high temperature PEMFC with CO tolerant catalysts.

Some studies reported in the literature have suggested the use of niobium as the second element in bimetallic catalysts. The first Nb-based electrocatalyst for fuel cell applications was prepared by Papageorgopoulos et al. [16]. The presence of Nb increased the CO tolerance of Pt/C and PtRu/C electrocatalysts. Indeed, the best result was obtained for a Pt_9Nb/C catalyst. They reported that larger Nb contents favoured the formation of oxy-hydorxy species that impaired the hydrogen oxidation process. Later, Ueda et al. [17] added again niobium in the form of NbO_x to unsupported and carbon-supported Pt and unsupported and carbon-supported PtRu electrocatalysts. They observed an enhanced CO tolerance reflected by a smaller CO onset potential in electrochemical CO stripping experiments. The enhancement was attributed to a strong electronic effect that reduced the amount of poisoned Pt sites with CO. Atanassov and co-workers [18] recently published a study showing a beneficial effect of a mixed Nb and Ru oxide ($NbRu_yO_z$) on the ethanol oxidation process, especially for cleaving the C–C bond. Rocha et al. [19] also reported a larger ethanol electro-oxidation performance for PtNb/C-based electrocatalysts. Orilall et al. [20] displayed an enhanced activity for Pt and PtPb deposited onto niobium oxide/carbon mesoporous structure for formic acid electro-oxidation. Recently, Justin et al. [21] developed a Pt–Nb_2O_5/C catalyst with an enhanced activity for methanol electro-oxidation. They attributed the beneficial effect to the easily reducible Nb_2O_5, donating –OH species to the CO-poisoned Pt sites, aside from strong metal support interactions between Pt and Nb_2O_5. It is interesting to note here that Nb_2O_5 has shown activity for selective oxidation of CO in $H_2 + CO$ streams [22–27], postulating it as a promising auxiliary secondary metal in processes where CO-adsorbed species are involved. Also, niobium-based materials have been used in the cathode. In general, addition of niobium improves the long-term stability of the support, especially when combined with TiO_2 [28–34], showing a reduced corrosion rate compared to standard carbon black materials (Vulcan XC-72R). In other cases, especially when Nb suboxides are used, an enhancement in the oxygen reduction reaction activity has been reported [31–36]. Again, the electronic effect and lateral repulsions between oxy-hydroxy Nb species and Pt–OH promote the activity for the oxygen reduction reaction of Pt–NbO_x/C electrocatalysts.

With these antecedents, the combination of platinum and niobium could be an attractive option as anode catalyst in PEM fuel cells fed with CO containing hydrogen. Thus, this study aims at analysing the effect of the addition of niobium to platinum in order to develop a CO tolerant catalyst. Different PtNb catalysts were prepared, physically and morphologically characterised and tested electrochemically in a half-cell (three electrode glass cell) first, and then in an actual fuel cell device, operating on the traditional Nafion® membranes (low temperature), and on the alternative ABPBI membrane impregnated with phosphoric acid at high temperature. Finally, the electrochemical behaviour of the system was studied when feeding pure CO/O_2 at different temperatures in order to achieve a deeper understanding of the CO tolerance mechanism.

2 Experimental

2.1 Catalysts preparation

Platinum–niobium catalysts supported on Vulcan XC-72R carbon black were prepared by reduction of the salt precursors. In a typical procedure, the required amount of hexachloroplatinic acid ($H_2PtCl_6{\cdot}6H_2O$, Sigma Aldrich) was dissolved in water, whereas niobium pentachloride ($NbCl_5$, Sigma Aldrich) was dissolved in ethanol. Then, the precursor solutions were simultaneously added to the reaction medium that contained the appropriate amount of carbon in 100 ml of 2 mol l^{-1} formic acid previously heated at 80 °C. The system was kept under vigorous stirring at this temperature for 1 h, and then left for 12 h without heating in order to guarantee the complete reduction/deposition of the two metals on the carbon. Next, the mixture was filtered, washed thoroughly with ultrapure water (obtained from a Milli-Q water filtration station, Millipore), and dried in an oven for 1 h at 80 °C. Further details about the experimental procedure can be found elsewhere [37]. For all the catalysts, 200 mg were prepared with a nominal metallic percentage of 20 %.

2.2 Catalyst characterisations

2.2.1 Physical and morphological characterisation

The chemical composition of the catalysts, in particular the Pt:Nb ratio, was determined by means of a Zeiss-Leica/440 SEM microscope equipped with an energy-dispersive spectrometer (EDS). The actual metal percentage was evaluated by thermal treatment of the samples in an air atmosphere at 800 °C for 3 h. By this, it is possible to burn the carbon support, remaining the metal oxides (PtO_2 and Nb_2O_5). Powder X-Ray diffraction (XRD) patterns were recorded on a Rigaku Ultima IV (Rigaku Corp., Japan) from 20° to 90° (0.02° step, 2° min^{-1}) in order to determine the presence of crystalline phases and the mean crystal size. Finally, the nanometric structure of the catalysts was explored by transmission electron microscopy (TEM) on a FEI-TECNAI G2F20 microscope operating at 200 kV.

2.2.2 Electrochemical characterisation

The different catalysts were first characterised electrochemically by cyclic voltammetry. A suspension of the catalyst (1 mg) on isopropyl alcohol was prepared and dispersed with the aid of an ultrasonic bath. With the aid of a chromatographic syringe, the suspension was carefully deposited on the electrode until completing 40 µl, corresponding to a platinum loading of approximately 100 µg cm^{-2}. Once dried, the electrode was inserted into a three-electrode glass cell containing a 0.5 mol l^{-1} H_2SO_4 solution. A reference hydrogen electrode (RHE) was prepared by electrolysis in the same electrolyte support. Previous to the cyclic voltammetry experiment, the system was purged with argon in order to remove oxygen, and next it was cycled between ≈70–800 mV several times until obtaining a stable voltammogram.

CO stripping was also carried out. The working electrode was polarised at 50 mV and CO was bubbled for 10 min in order to get complete adsorption on the catalyst surface. Then, the system was purged with argon in order to remove any CO dissolved in the solution. Once the preparation procedure was concluded, the system was cycled between 50 and 1200 mV three times: the actual CO stripping was recorded in the first cycle and the baseline was established by the last one. The electrochemically active surface area was determined by assuming a charge of 420 µC cm^{-2} for a monolayer of carbon monoxide adsorbed on the electrochemically active catalytic surface.

2.3 Fuel cell experiments

2.3.1 Preparation of the membrane-electrode-assembly (MEA) for Nafion®-based PEMFC

Nafion®-based gas diffusion electrodes (GDE) were prepared as follows. A diffusion layer was prepared with carbon powder (Vulcan XC-72R) and 15 wt% PTFE (TE-3893, Dupont), and applied homogenously over a carbon cloth (PWB-3, Stackpole) by vacuum filtration. On top of this layer, a catalyst ink was applied by brushing. Its composition consisted of the catalyst, Nafion® emulsion (5 % in aliphatic alcohols) in an amount of 35.5 % with respect to the total catalyst weight and isopropyl alcohol as solvent. The total platinum loading deposited was 0.5 mg cm^{-2}. The electrodes were next dried in an oven at 80 °C for 1 h. The geometric area was 4.62 cm^2. The same procedure was followed for the preparation of both electrodes. The different catalysts were prepared with three compositions of PtNb/C (see Table 1) and commercial E-TEK Inc. 20 % Pt/C.

A Nafion® 115 membrane was used as electrolyte in the MEA. The membrane was previously pre-treated with hot hydrogen peroxide (3 vol.%) and hot sulphuric acid in order to remove any organic and metallic residues within the membrane [38]. The membrane was sandwiched between the electrodes, and a pressure of 5 tons was applied at 125 °C for 2 min.

2.3.2 Preparation of the membrane-electrode-assembly (MEA) for ABPBI-based PEMFC

ABPBI-based GDEs were prepared as follows. On the same type of gas diffusion layer, it was brush-spread a

Table 1 Actual composition and metal content of the different prepared catalysts

Catalyst	Nominal Pt:Nb ratio	Actual Pt:Nb ratio (confidence interval)	% of metal in the catalyst
PtNb/C	50:50	73:27 (± 5)	17
Pt_2Nb/C	67:33	94:6 (± 2)	17
Pt_3Nb/C	75:25	99:1 (± 0.7)	18

thick ink composed of the catalyst, PTFE (10 wt% referred to the carbon loading) and isopropyl alcohol as solvent. Once the required amount of catalyst (0.5 mg cm^{-2} of platinum for both electrodes) was applied, the electrodes were dried in an oven at 120 °C in order to evaporate any residual solvent. Electrodes were prepared with the $Pt_{94}Nb_6/C$ and commercial E-TEK 20 % Pt/C catalysts.

The ABPBI membrane was prepared according to the procedure described elsewhere [39], and immersed in an 80 wt% phosphoric acid bath for at least 3 days in order to guarantee the complete impregnation. Before preparing the MEA, the membrane was taken out from the doping bath, and wiped out with filter paper in order to remove the excess acid from the surface. Then, the membrane was placed between the electrodes, and hot-pressed at 150 °C and 1 ton for 15 min. Finally, the MEA was stored in a sealed plastic bag until future use in the fuel cell.

2.3.3 Fuel cell measurements

The Nafion®-based MEA was operated at 85 °C. In order to maintain an adequate level of humidification of the MEA that ensures a good conductivity, both the anode and the cathode gaseous streams were humidified by bubbling in water chambers at, in the case of the anode, 100 °C, and in the case of the cathode, 90 °C. The dry volumetric flows were 0.2 l min^{-1} for both gases. Pure hydrogen or hydrogen containing 100 ppm of CO, and oxygen were used as fuel and comburent, respectively. Backpressure was applied for both anode (0.1 MPa) and cathode (0.07 MPa) streams for correction of the water vapour pressure. The ABPBI-based MEA was operated at 130 and 190 °C. No pre-humidification was required for operation, using the same volumetric flows than in the case of Nafion®. Due to the expected higher tolerance of the ABPBI system, hydrogen containing 2 % of CO was used instead for the CO tolerance measurements. Final tests were carried out with pure carbon monoxide and oxygen in the same experimental setup and conditions than in the ABPBI tests.

The experimental rig consisted of two carbon monopolar plates, into which a four-channel serpentine geometry was machined. Within the carbon plates, heating rods were fitted. The temperature was controlled with the aid of a temperature controller (Flyever). The voltage probes were drilled into the carbon plates. The endplates were made of aluminium, and a compressible carbon foil was inserted in-between in order to improve the electrical contact. The current collectors were placed in both endplates.

The polarisation curves were recorded galvanostatically for both types of cells. The system was polarised at a fixed current with the aid of an electronic load, and the voltage was recorded after stabilisation. The polarisation curves were recorded from the open circuit voltage (OCV) in growing current steps. The measurements were repeated three times, reporting the average values of the voltage.

3 Results and discussion

3.1 Structural and morphological characterisation

The actual compositions of the prepared catalysts are collected in Table 1 referred to the Pt:Nb ratio and the total metal content. As it can be seen, the actual amount of deposited niobium on the catalysts was significantly lower than the nominal (expected from the precursors concentration). Although no clear reasons were found for explaining this behaviour, when niobium pentachloride, dissolved in ethanol, is added to the reduction medium, some niobium oxide nanoparticles might form as a consequence of the hydrolysis of the chloride [40, 41], without anchoring on the carbon support and percolating the filter paper. The most critical case corresponds to the Pt_3Nb_1/C, where only 1 % of niobium was detected. It is important to note that no platinum was detected in the supernatant after filtering the reaction medium for preparation of the catalysts. The amount of metal present (after subtracting the contribution of oxygen in the oxides) in all the samples was 17–18 % according to the losses of niobium, in agreement with the nominal content considering the complete deposition of platinum and the metal ratio. From now on, the catalysts will be identified by their actual content.

XRD patterns of the different catalysts are shown in Fig. 1. Typical peaks associated to the different orientations of the Pt fcc crystal structure can be observed. No peaks associated to any Nb crystalline phase are present, and no shift of the Pt peaks was detected. By applying Scherrer's equation, it is possible to estimate the values of the crystal sizes. These are collected in Table 2, along with the lattice parameters. Crystal sizes were all in the nanometric range from 2.8 to 3.6 nm. No significant change was observed in this parameter, regardless of the presence of niobium, so it may be concluded that there was no insertion of this metal within the Pt crystalline structure. As a consequence, niobium is expected to be present as an

amorphous oxide phase or secondary segregated metallic phase. According to the literature, the most likely state under the synthesis conditions (aqueous medium) is in the form of niobium pentoxide due to the hydrolysis of the $NbCl_5$ [40–42].

TEM images of the different catalysts are displayed in Fig. 2. As it can be seen, metal nanoparticles deposited on the carbon support spread quite homogeneously on the carbon surface. Nevertheless, some small and big particles can be visualised, displaying some dispersion. This reflects on the corresponding histograms of the samples, collected in Fig. 3. Average particle sizes (d_n) (counting approx. 400 particles) were calculated by applying Eq. 1, where m_i is the number of particles with a diameter d_i. The corresponding values are collected in Table 2. As it can be seen, the mean particle sizes confirm the nanoparticle nature of the metal deposited on the carbon support. Moreover, the particle sizes for all the PtNb/C are between 2.4 and 2.6 nm, similar enough to disregard any effect associated to the particle size, especially in terms of the CO adsorption strength [43].

$$d_n = \frac{\sum_i m_i d_i}{\sum_i m_i} \quad (1)$$

3.2 Electrochemical characterisation

Cyclic voltammograms of the different catalysts are shown in Fig. 4 (normalised by the electrochemically active area from the CO stripping). As it can be seen, the three PtNb catalysts show the hydrogen adsorption/desorption regions with the peaks associated to the different crystalline faces exposed to the electrolyte [44]. It is significant the fact that the double layer capacitance does not grow despite the presence of the oxide. Both results differ from what it has been observed for other bimetallic materials [45], where the hydrogen adsorption/desorption region becomes a single hump and there is a significant increase in the double layer current. CO stripping profiles are displayed in Fig. 5 normalised by the own electrochemically active area from the CO stripping voltammograms. As it can be seen, there is a shift of the onset potential toward less positive values for CO oxidation on catalysts containing Nb. The corresponding values are collected in Table 3 (the onset potential was considered as the value of the potential when the slope of the voltammograms exceeded 0.005 mA cm^{-2} mV^{-1}). It is important to note that Nb by itself does not show any activity in terms of hydrogen adsorption/desorption and CO oxidation, as observed by cyclic voltammetry and CO stripping experiments using this material. The presence of niobium results beneficial to oxidise CO at lower potentials. Furthermore, the larger the niobium content in the catalysts, the larger the shift of the onset CO oxidation potential. This smaller potential is related to the better characteristics of the catalysts in terms of CO tolerance, and is expected to be beneficial for a fuel cell under operation with H_2 + CO fuel. Also, platinum active sites that were previously blocked by this poison get cleaned at smaller potentials than in the case of the Pt/C catalyst, which is of interest in terms of a more efficient fuel cell. This result is in agreement with others presented in the literature for $PtNbO_x$ systems [17, 21, 46].

Assuming that Nb is in the form of Nb_2O_5, the observed decrease in the CO onset potential can be explained in terms of the two basic mechanisms described in the literature: electronic effect and bifunctional mechanism. In the first case, the electronic interactions between platinum and niobium oxide induce a modification in the CO adsorption energy. Nb_2O_5 is well known for participating in strong metal support interactions, and indeed, this effect has been reported for platinum deposited on niobium oxide [21, 35]. The origin of these interactions lies in the oxygen vacancies present in the amorphous surface oxide [27, 47]. These vacancies may be able to trap electrons donated by platinum, which, in turn, would result in a weakening of the CO adsorption strength, facilitating its oxidation. The bifunctional mechanism is based on the donation of –OH species

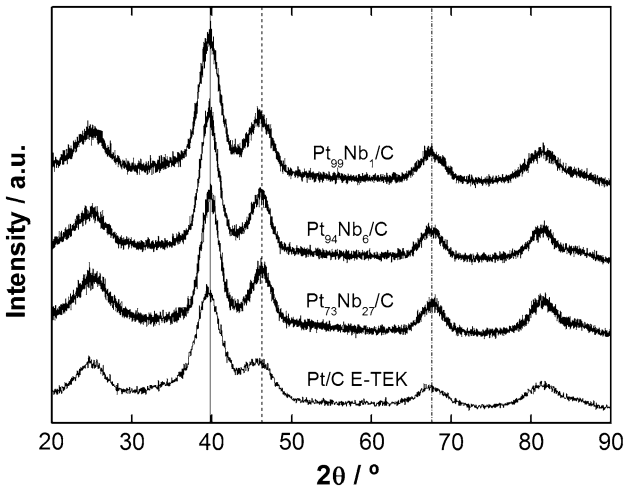

Fig. 1 XRD diffractograms of the carbon-supported PtNb catalysts prepared with different Nb contents

Table 2 Main parameters from XRD patterns

Catalyst	Crystal size (nm)	Lattice parameter (nm)	TEM mean particle size (nm)
Pt/C E-TEK	2.8	0.3927	
$Pt_{73}Nb_{27}/C$	3.5	0.3917	2.6
$Pt_{94}Nb_6/C$	3.6	0.3922	2.4
$Pt_{99}Nb_1/C$	3.2	0.3922	2.6

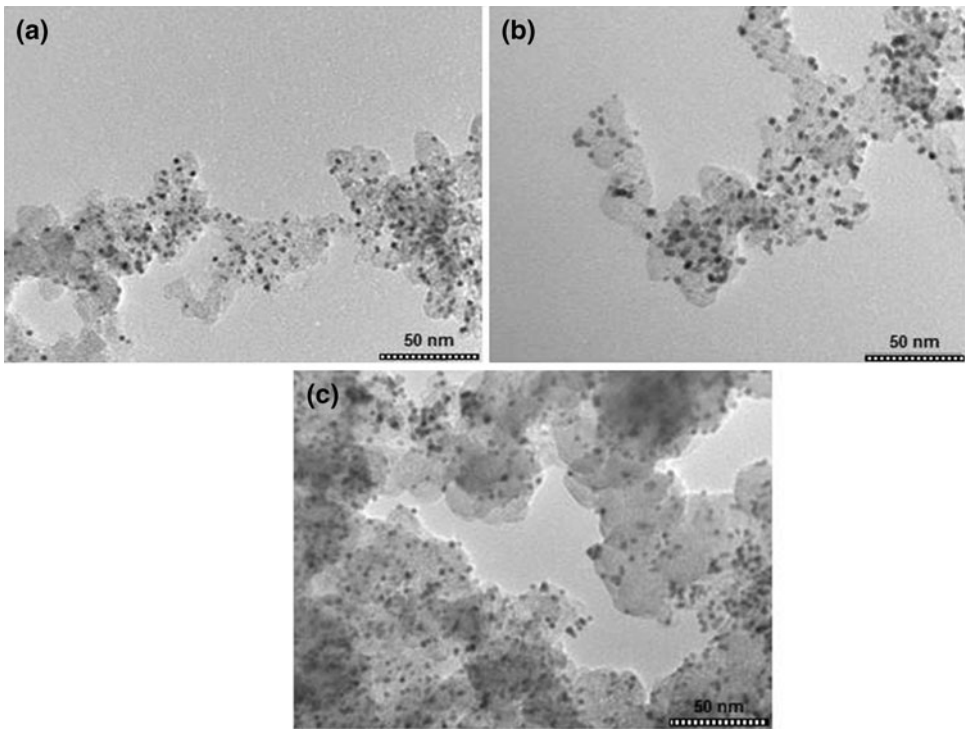

Fig. 2 TEM images of the carbon-supported PtNb catalysts prepared with different Nb contents: **a** $Pt_{73}Nb_{27}/C$, **b** $Pt_{94}Nb_6/C$, **c** $Pt_{99}Nb_1/C$

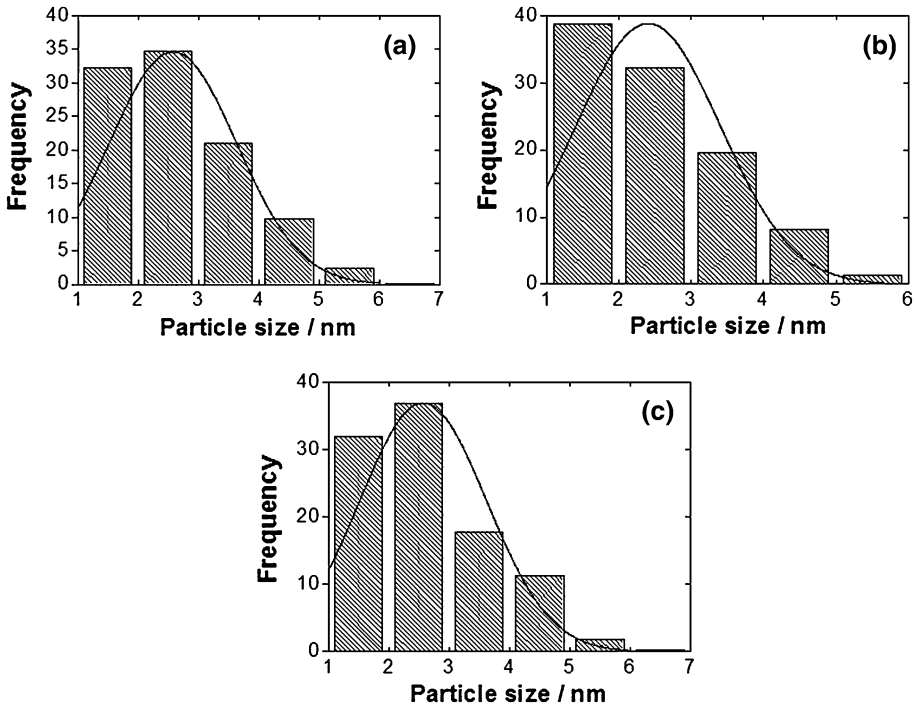

Fig. 3 Histograms of the carbon-supported catalysts prepared: **a** $Pt_{73}Nb_{27}/C$, **b** $Pt_{94}Nb_6/C$, **c** $Pt_{99}Nb_1/C$

to platinum sites from neighbouring reducible oxide species at lower potentials than those required for platinum oxidation. This behaviour has been already postulated for the $PtNb_2O_5$ system: niobium pentoxide is an easily reducible oxide that therefore can donate oxygenated species to the Pt–CO sites [46]. The combination of these two mechanisms results in a decrease of the CO oxidation onset potential, and indeed, the increase in the onset potential with the decrease of the Nb content can be explained by the smaller interface between the platinum and the niobium pentoxide sites. Nevertheless, it is very relevant that even the catalyst with 1 at.% Nb shows a decrease in the onset potential. The bifunctional mechanism requires a high interfacial area between the two components in order to

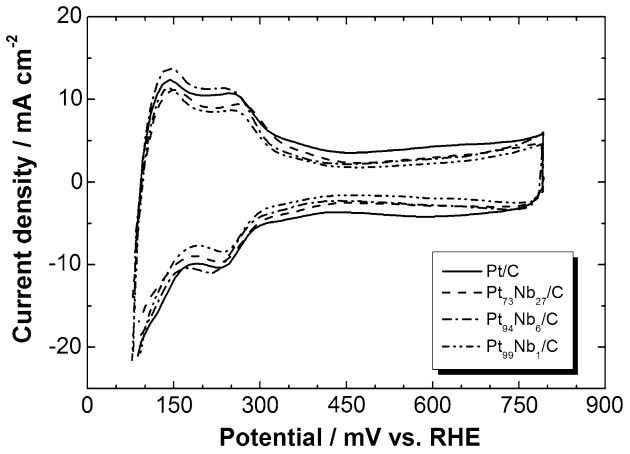

Fig. 4 Cyclic voltammograms of the carbon-supported PtNb and Pt catalysts (normalised by the electrochemically active area from the CO stripping)

fully act. The 1 at.% Nb catalyst does not fulfil this, so the interaction that supports the decrease in the onset potential should be a very strong electronic effect between Pt and Nb_2O_5 that weakens the adsorption strength of CO on the Pt sites. For the larger Nb contents, the electronic effect becomes more intense along with the more noticeable bifunctional effect, further reducing the CO oxidation onset potential.

3.3 Fuel cell performance

3.3.1 Operation on Nafion®-based PEMFC

The fuel cell performances with Nafion® membrane for the different catalysts are shown in Fig. 6a. For operation under hydrogen, it is only displayed the polarisation curve corresponding to Pt/C, since the curves for the other three

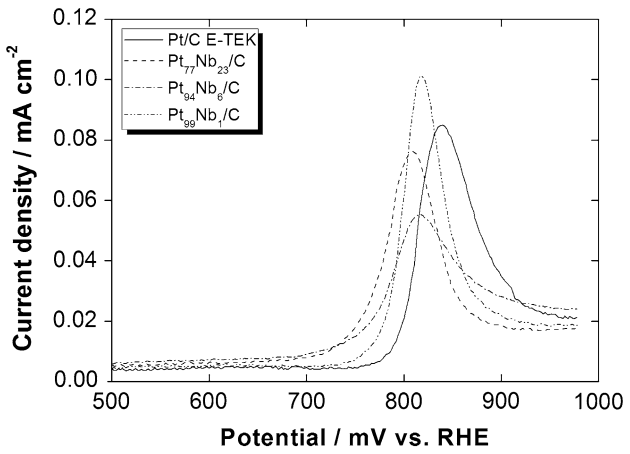

Fig. 5 CO stripping of the carbon-supported PtNb and Pt catalysts (normalised by the electrochemically active area from the CO stripping)

Table 3 Onset potential for CO oxidation

Catalyst	Onset potential for CO oxidation (mV)
Pt/C E-TEK	786
$Pt_{73}Nb_{27}/C$	739
$Pt_{94}Nb_6/C$	752
$Pt_{99}Nb_1/C$	771

catalysts largely resemble this one. In the case of operation under hydrogen with 100 ppm CO, there are noticeable differences between the curves. Anodes composed by Pt and Nb present a better performance compared to pure platinum, confirming the enhanced CO tolerance of these materials. It is significant the steep decay in the cell performance for the Pt/C catalyst above 90 mA cm^{-2}. Such behaviour is typical of Pt when poisoned by CO, due to the active sites blocked by the monoxide. This limits the performance of the catalyst, which just recovers at low cell

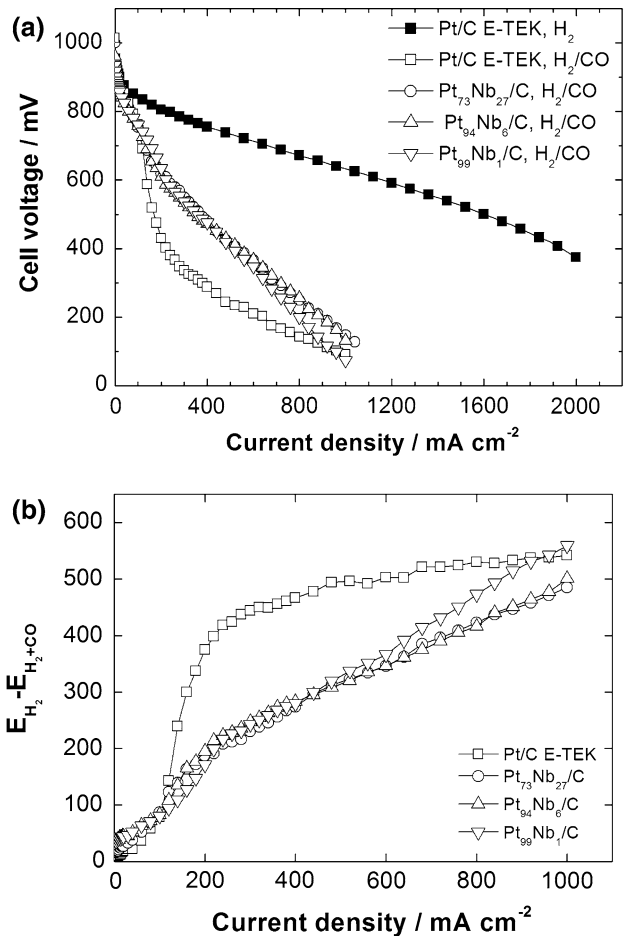

Fig. 6 **a** Polarisation curves of the different catalyst operating on H_2 and H_2 + CO, **b** overpotential associated to the substitution of pure H_2 by H_2 + CO. System operating on Nafion® membrane at 80 °C

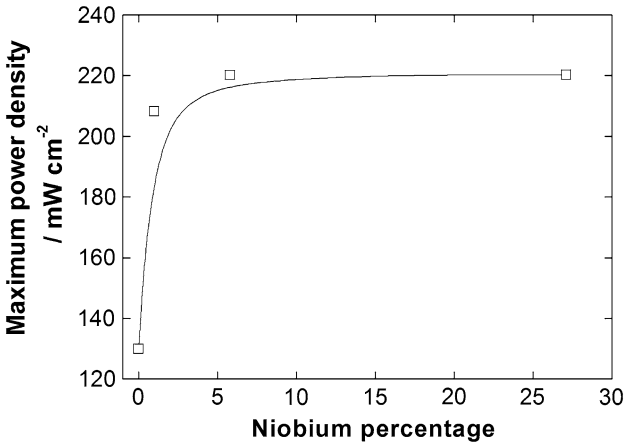

Fig. 7 Maximum power density drawn from the Nafion®-based fuel cell for different niobium contents

voltages (high anodic overpotentials) when the formation of surface Pt–OH species starts [47]. In the case of the PtNb/C catalysts, that decay was not observed. This can be more clearly observed in Fig. 6b, where the beneficial effects of the niobium on the catalysts reflects on the lower overpotential associated to the introduction of CO in the fuel stream, expressed as $E_{H_2} - E_{H_2+CO}$. Hence, the presence of Nb ameliorates the poisoning effect of the carbon monoxide. The maximum power densities drawn from the cell clearly confirm the significant enhancement obtained when niobium is present in the catalyst formulation (Fig. 7). In agreement with the CO stripping results, the catalyst with a low Nb content already shows a significant enhancement in the cell performance under the presence of carbon monoxide, confirming the existence of significant electronic interactions between Pt and Nb_2O_5. Finally, it is very significant the almost imperceptible increase in the maximum power density when the Nb content increases from 6 to 23 % under operation with carbon monoxide. This can be explained in terms of a governing mechanism for the enhanced CO tolerance based on the electronic effect, which seems to be fully developed with low Nb contents. Moreover, this result implies that the electronic effect has the most significant contribution to the greater CO tolerance.

This result is rather significant since, as far as the authors know, this is the first report of the fuel cell performances with a platinum–niobium electrocatalysts using $H_2 + CO$ as fuel. Previous reports (Papageorgopoulos et al. [16] and Ueda et al. [17]) showed promising features of this catalyst based mainly on CO stripping results, and only Ref. [16] collects some preliminary fuel cell data. However, none of them showed polarisation curves. References [21] and [45] show the fuel cell performance for direct methanol fuel cells, displaying an enhancement in the methanol electro-oxidation reaction, along with CO stripping results that suggest the suitability of Nb_2O_5 for increasing the CO tolerance.

3.3.2 *Operation on ABPBI-based PEMFC*

The polarisation curves for Pt/C and $Pt_{94}Nb_6$/C catalysts used in an ABPBI-based PEMFC are depicted in Fig. 8 at

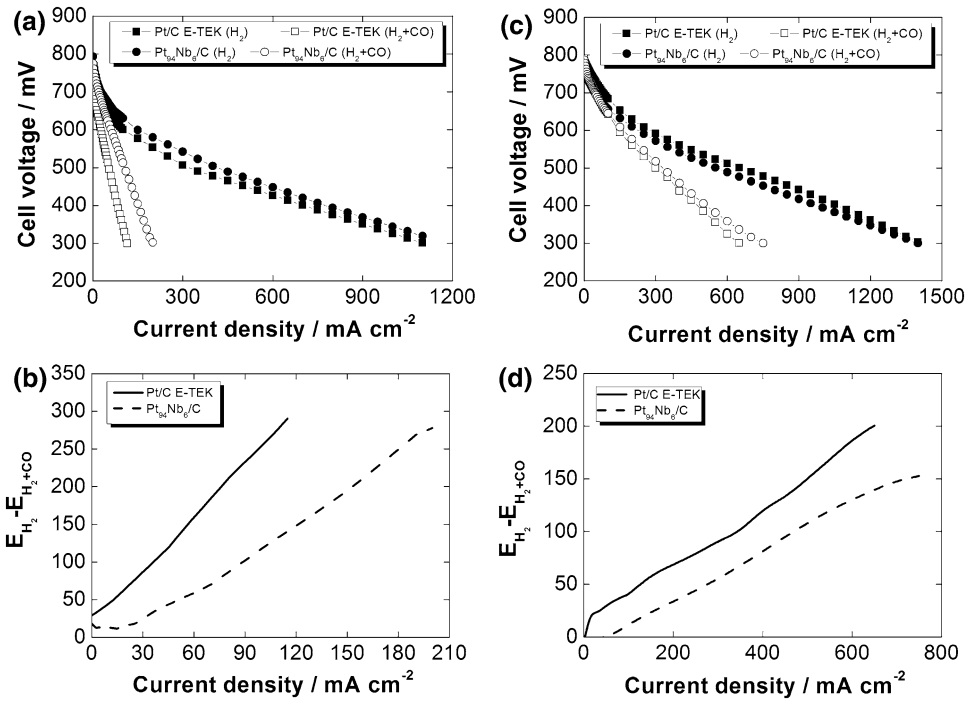

Fig. 8 **a** Polarisation curves for the different catalysts at 130 °C, **b** overpotential associated to the substitution of pure H_2 by $H_2 + CO$ at 130 °C, **c** polarisation curves for the different catalysts at 190 °C, **d** overpotential associated to the substitution of pure H_2 by $H_2 + CO$ at 190 °C. ABPBI membrane

130 and 190 °C. In this case, the CO concentration in the fuel stream was 2 % (corresponding to 20,000 ppm). The $Pt_{94}Nb_6$/C catalyst was chosen since it already showed a good tolerance for CO when used in the Nafion® system despite the presence of only 6 at.% niobium. The temperature of 130 °C was intentionally chosen since it is expected to reflect the most severe CO poisoning effects, as opposed to 190 °C.

As it can be seen, the polarisation curves when operating on hydrogen are similar for both catalysts independently of the temperature. However, when operating on H_2 + CO, there exists a significant drop in the cell performance, more deleterious at 130 than at 190 °C. Nonetheless, the decay is lower in the case of the PtNb/C catalyst, confirming the higher tolerance of the catalyst when Nb is present in its formulation. As in the previous section the overpotential associated to the introduction of CO in the fuel was calculated for the two temperatures. At 130 °C, the beneficial effect of the presence of Nb is rather noticeable, with a difference in the overpotential associated to the addition of CO of 130 mV at 100 mA cm^{-2} (comparing $Pt_{94}Nb_6$/C vs. Pt/C E-TEK). At 190 °C, that difference is 30 mV, reflecting that at this temperature the CO tolerance is less sensitive to the catalyst composition, even though the $Pt_{94}Nb_6$/C still performs better than the Pt/C catalyst. This lower CO tolerance with increasing temperature was also reported by Modestov et al. [48], where they observed that the beneficial effect of the presence of ruthenium diminishes with the temperature.

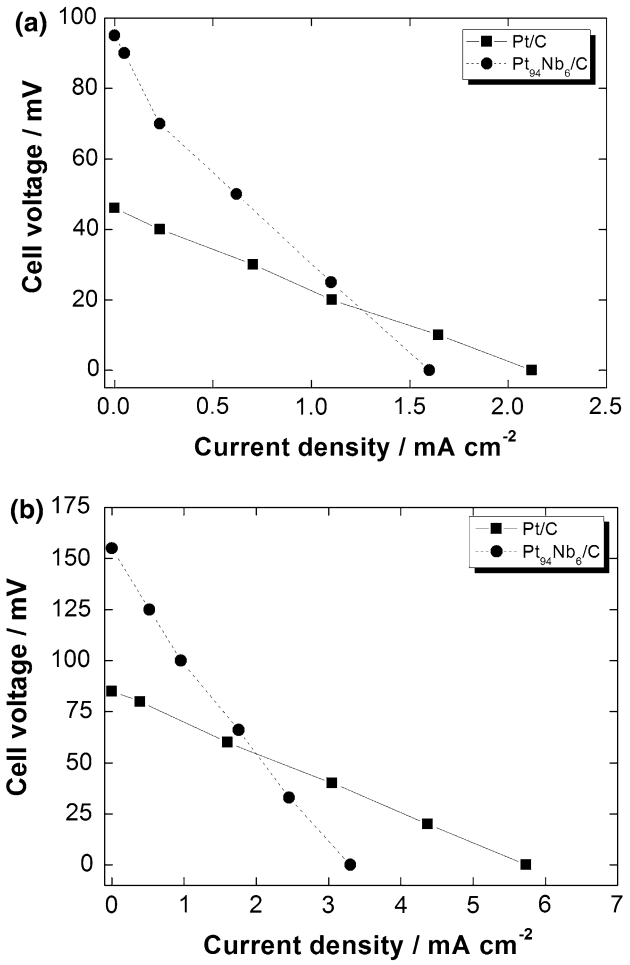

Fig. 9 Polarisation curves for the different catalysts operating in a CO/O_2 cell at **a** 130 °C, and **b** 190 °C

This result shows for the first time the application of a platinum–niobium-based catalyst in high temperature PEMFC systems. It can be considered very important from a practical point of view, especially looking at applications in which the PEMFC are coupled with a reforming system, using as fuel, for example, ethanol. A high CO tolerance will allow a less stringent and costly hydrogen cleaning system from a less demanding requirement for CO concentration reduction (tens of ppm for Nafion®-based PEMFC versus thousands of ppm for high temperature-ABPBI-based PEMFC). As a consequence, the combination of a more CO-tolerant catalyst, along with the increase in the operational temperature could lead to a more adequate coupling between a hydrocarbon reforming system and a fuel cell.

3.3.3 Operation on CO/O_2

Finally, in order to better visualise the effect of the Nb on the CO electro-oxidation behaviour of the catalysts, polarisation curves on an ABPBI-based fuel cell operating with CO/O_2 are displayed in Fig. 9 at 130 and 190 °C.

Two facts can be noticed due to the presence of niobium: an increase in the open circuit voltage of the cell and a decrease of the maximum electro-oxidation current. This can be explained in terms of the weakening of Pt–CO bond ascribed to the electronic effect of Nb on platinum, promoting the CO electro-oxidation at lower anodic potentials, in agreement with the CO stripping results, and hence, increasing the open circuit voltage of the system. On the other hand, the weakening of the Pt–CO bond does not favour the electro-oxidation current. This can be explained in terms of the lower coverage of CO on the platinum surface, owing to the electronic effect of Nb [16, 17, 26, 35, 49, 50], limiting the maximum current density. These results are in agreement with those of Sect. 3.1, and confirm the importance of the electronic effect that Nb exerts on platinum. A pure bifunctional process would have led to an increase in the open circuit voltage as well as in the current density for CO electro-oxidation, associated to the more liable donation of –OH groups. Also, such a low Nb content does not seem to be sufficient for the development of a bifunctional effect across the platinum surface.

4 Conclusions

From this study, the following conclusions can be drawn:

- The inclusion of niobium, most likely in the form of Nb_2O_5, as secondary element in platinum electrocatalysts exerts a positive effect in the CO tolerance even when low amounts are present. A decreased CO onset potential and, more significantly, an enhanced fuel cell performance under $H_2 + CO$ fuel, both in low (in a Nafion®-based PEMFC) and in high (ABPBI-based PEMFC) temperature systems, support this.
- In this sense, fuel cell results, obtained systematically for the first time, reveal that the most suitable catalyst is the $Pt_{94}Nb_6/C$, which shows reduced CO overpotentials in low temperature systems when using 100 ppm CO in the hydrogen stream, and in high temperature systems when using a large 2 vol.% CO.
- The Nb promotional effect comes from very strong metal support interactions between Pt and Nb_2O_5 that weaken the Pt–CO adsorption strength, reducing the CO coverage and facilitating its oxidation at lower potentials. This opens the possibility of using low Nb_2O_5 loadings for improving the CO tolerance.
- Despite the bifunctional mechanism can assist in promoting the CO tolerance, it is not the governing effect.
- Finally, niobium can be considered as a suitable secondary component in the development of strategic PEMFC CO-tolerant anodes.

Acknowledgments Authors want to thank to the Fundação de Amparo à Pesquisa do Estado de São Paulo (FAPESP), the Conselho Nacional de Desenvolvimento Científico e Tecnológico (CNPq), and the Coordenação de Aperfeiçoamento de Pessoal de Nível Superior (CAPES) for the financial support. In particular, Thairo A. Rocha thanks to the CNPq (Proc. 142146/2012-9) for a Master Degree scholarship, and José J. Linares thanks FAPESP for a post-doctoral fellowship (Proc. 2010/07108-3).

References

1. Ellis MW (2001) Fuel cell systems: efficient, flexible energy conversion for the 21st century. Proc IEEE 89:1808–1818
2. Thomas CE (2008) Fuel cell and battery electric vehicles compared H2Gen Innovations, Inc. Alexandria, Virginia. http://www1.eere.energy.gov/hydrogenandfuelcells/education/pdfs/thomas_fcev_vs_battery_evs.pdf. Accessed 15 Oct 2012
3. His S (2003) Hydrogen: an energy vector for the future? Panorama 2004
4. Wurster R, Schindler J. (2010) Solar and wind energy coupled with electrolysis and fuel cells. Handbook of fuel cells, John Wiley & Sons, West Sussex, UK
5. Vaidya PD, Rodrigues AE (2006) Insight into steam reforming of ethanol to produce hydrogen for fuel cells. Chem Eng J 15:39–49
6. Xie D, Zhang E, Li R, Zhang Y (2012) Syngas CO cleaning for fuel cell applications by preferential oxidation: catalyst development and reactor design. Int J Low-Carbon Tech doi:10.1093/ijlct/cts056
7. Pereira LGS, Paganin VA, Ticianelli EA (2009) Investigation of the CO tolerance mechanism at several Pt-based bimetallic anode electrocatalysts in a PEM fuel cell. Electrochim Acta 54:1992–1998
8. Ciapina EG, Gonzalez ER (2009) Investigation of the electrooxidation of CO on Pt-based carbon supported catalysts ($Pt_{75}Sn_{25}/C$, $Pt_{65}Ru_{35}/C$ and Pt/C) by electrochemical impedance spectroscopy. J Electroanal Chem 626:130–142
9. Nepel TCM, Lopes PP, Paganin VA, Ticianelli EA (2013) CO tolerance of proton exchange membrane fuel cells with Pt/C and PtMo/C anodes operating at high temperatures: a mass spectrometry investigation. Electrochim Acta 88:217–224
10. Pereira LGS, dos Santos FR, Pereira ME, Paganin VA, Ticianelli EA (2006) CO tolerance effects of tungsten-based PEMFC anodes. Electrochim Acta 51:4061–4066
11. Santiago EI, Giz MJ, Ticianelli EA (2003) Studies of carbon monoxide oxidation on carbon-supported platinum–osmium electrocatalysts. J Solid State Electrochem 7:607–613
12. Li Q, He R, Gao J-A, Jensen JO, Bjerrum NJ (2003) The CO poisoning effect in PEMFCs operational at temperatures up to 200°C. J Electrochem Soc 150:A1599–A1605
13. Bose S, Kuila T, Nguyen TXH, Kim NH, Lau K-T, Lee JH (2011) Polymer membranes for high temperature proton exchange membrane fuel cell: recent advances and challenges. Prog Polym Sci 36:813–843
14. Linares JJ, Sanches C, Paganin VA, Gonzalez ER (2012) Poly(2,5-bibenzimidazole) membranes: physico-chemical characterization focused on fuel cell applications. J Electrochem Soc 159:F194–F202
15. Lobato J, Cañizares P, Rodrigo MA, Linares JJ, Manjavacas G (2006) Synthesis and characterisation of poly[2,2-(*m*-phenylene)-5,5-bibenzimidazole] as polymer electrolyte membrane for high temperature PEMFCs. J Membr Sci 280:351–362
16. Papageorgopoulos DC, Keijzer M, de Bruijin FA (2002) The inclusion of Mo, Nb and Ta in Pt and PtRu carbon supported electrocatalysts in the quest for improved CO tolerant PEMFC anodes. Electrochim Acta 48:197–204
17. Ueda A, Yamada Y, Ioroi T, Fujiwara N, Yauda K, Miyazaki Y, Kobayashi T (2003) Electrochemical oxidation of CO in sulfuric acid solution over Pt and PtRu catalysts modified with TaO_x and NbO_x. Catal Today 84:223–229
18. Konopka DA, Li M, Artyushkova K, Marinkovic N, Sasaki K, Adzic R, Ward TL, Atanassov P (2011) Platinum supported on NbRuyOz as electrocatalyst for ethanol oxidation in acid and alkaline fuel cells. J Phys Chem C 115:3043–3056
19. Rocha TA, Linares JJ, Colmati F, Ciapina EG, González ER (2012) Electrocatalytic activity of platinum–niobium nanoparticles for ethanol oxidation. J Electrochem Soc 159:F650–F658
20. Orilall MC, Matsumoto F, Zhou Q, Sai H, Abruña HD, DiSalvo FJ, Wiesner U (2009) One-pot synthesis of platinum-based nanoparticles incorporated into mesoporous niobium oxide–carbon composites for fuel cell electrodes. J Am Chem Soc 131:9389–9395
21. Justin P, Hari Krishna Charan P, Ranga Rao G (2010) High performance Pt–Nb_2O_5/C electrocatalysts for methanol electrooxidation in acidic media. Appl Catal B: Environ 100:510–515
22. Aranda DAG, Ramos AD, Passos FB, Schmal M (1996) Characterization and dehydrogenation activity of Pt/Nb_2O_5 catalysts. Catal Today 28:119–125
23. Passos FB, Aranda DAG, Soares RR, Schmal M (1998) Effect of preparation method on the properties of Nb_2O_5 promoted platinum catalysts. Catal Today 43:3–9

24. Schmal M, Aranda DAG, Soares RR, Noronha FB, Frydman A (2000) A study of the promoting effect of noble metal addition on niobia and niobia alumina catalysts. Catal Today 57:169–176
25. Guerrero S, Miller JT, Wolf EE (2007) Activity and selectivity control by niobium for the preferential oxidation of co on pt supported catalysts. Appl Catal A 328:27–34
26. Uchijima T (1996) SMSI effect in some reducible oxides including niobia. Catal Today 28:105–117
27. Marques P, Ribeiro NFP, Schmal M, Aranda DAG, Souza MMVM (2006) Selective CO oxidation in the presence of H2 over Pt and Pt–Sn catalysts supported on niobia. J Power Sources 158:504–508
28. Zhang L, Wang L, Holt CMB, Zahiri B, Li Z, Malek K, Navessin T, Eikerling MH, Mitlin D (2012) Highly corrosion resistant platinum–niobium oxide–carbon nanotube electrodes for the oxygen reduction in PEM fuel cells. Energy Environ Sci 5:6156–6172
29. Tripković V, Abild-Pedersen F, Studt F, Cerri I, Nagami T, Bligaard T, Rossmeisl J (2012) Metal oxide-supported platinum overlayers as proton-exchange membrane fuel cell cathodes. ChemCatChem 4:228–235
30. Bauer A, Hui R, Ignaszak A, Zhang J, Jones DJ (2012) Application of a composite structure of carbon nanoparticles and Nb–TiO_2 nanofibers as electrocatalyst support for PEM fuel cells. J Power Sources 210:15–20
31. Sun S, Zhang G, Sun X, Cai M, Ruthkosky M (2012) Highly stable and active Pt/Nb-TiO_2 carbon-free electrocatalyst for proton exchange membrane fuel cells. J Nanotechnol 2012:8
32. Bauer A, Chevallier L, Hui R, Cavaliere S, Zhang J, Jones D, Rozière J (2012) Synthesis and characterization of Nb-TiO_2 mesoporous microsphere and nanofiber supported Pt catalysts for high temperature PEM fuel cells. Electrochim Acta 77:1–7
33. Bonakdarpour A, Tucker RT, Fleischauer MD, Beckers NA, Brett MJ, Wilkinson DP (2012) Nanopillar niobium oxides as support structures for oxygen reduction electrocatalysts. Electrochim Acta 85:492–500
34. Wang Y-J, Wilkinson DP, Guest A, Neburchilov V, Baker R, Nan F, Botton GA, Zhang J (2013) Synthesis of Pd and Nb–doped TiO_2 composite supports and their corresponding Pt–Pd alloy catalysts by a two-step procedure for the oxygen reduction reaction. J Power Sources 221:232–241
35. Sasaki K, Zhang L, Adzic RR (2008) Niobium oxide-supported platinum ultra-low amount electrocatalysts for oxygen reduction. Phys Chem Chem Phys 10:159–167
36. Senevirathne K, Hui R, Campbell S, Ye S, Zhang J (2012) Electrocatalytic activity and durability of Pt/NbO_2 and Pt/Ti_4O_7 nanofibers for PEM fuel cell oxygen reduction reaction. Electrochim Acta 59:538–547
37. Pinheiro ALN, Oliveira-Neto A, de Souza EC, Perez J, Paganin VA, Ticianelli EA, Gonzalez ER (2003) Electrocatalysis on noble metal and noble metal alloys dispersed on high surface area carbon. J New Mater Electrochem Sys 6:1–8
38. Smit MA, Ocampo AL, Espinosa-Medina MA, Sebastián PJ (2003) A modified Nafion membrane with in situ polymerized polypyrrole for the direct methanol fuel cell. J Power Sources 124:59–64
39. Linares JJ, Sanches C, Paganin VA, Gonzalez ER (2011) Poly(2,5-benzimidazole) membranes: physico-chemical characterization and high temperature PEMFC application. ECS Trans 41:1579–1593
40. Kai T, Matsumura T, Takahashi T (1992) The effect of support structure on CO_2 hydrogenation over a rhodium catalyst supported on niobium oxide. Catal Lett 16:129–135
41. Alquier C, Vandenborre MT, Henry M (1986) Synthesis of niobium pentoxide gels. J Non-Cryst Solids 79:383–395
42. Therwil K, Hooper J (1964) Process for the manufacture of niobium pentoxide or tantalum pentoxide. US Patent 3,133,788
43. Maillard F, Savinova ER, Stimming U (2007) CO monolayer oxidation on Pt nanoparticles: further insights into the particle size effects. J Electroanal Chem 599:221–232
44. Li H, Lee K, Zhang J (2008) Electrocatalytic H_2 oxidation reaction. In: Zhang J (ed) PEM fuel cell electrocatalysts and catalyst layers. Fundamentals and applications, 1st edn. Springer, London, p 145
45. Vidaković T (2005) Kinetics of methanol electrooxidation on PtRu catalysts in a membrane electrode assembly. Doctorate Thesis. Otto-von-Guericke-Universität Magdeburg
46. Chun H-J, Kim DB, Lim D-H, Lee W-D, Lee H-I (2010) A synthesis of CO-tolerant Nb_2O_5-promoted Pt/C catalyst for direct methanol fuel cell; its physical and electrochemical characterization. Int J Hydrogen Energy 35:6399–6408
47. Birss VI, Chang M, Segal J (1993) Platinum oxide film formation-reduction: an in situ mass measurement study. J Electroanal Chem 355:181–191
48. Modestov AD, Tarasevich MR, Filimonov VY, Davydova ES (2010) CO tolerance and CO oxidation at Pt and Pt–Ru anode catalysts in fuel cell with polybenzimidazole–H_3PO_4 membrane. Electrochim Acta 55:6073–6080
49. Tauster SJ (1987) Strong metal-support interactions. Acc Chem Res 20:389–394
50. Aranda DAG, Schmal M (1997) Ligand and geometric effects on Pt/Nb_2O_5 and Pt–Sn/Nb_2O_5 catalysts. J Catal 171:398–405